PERFORMANCE ASSESSMENT OF VARIOUS PV MODULE TYPES UNDER DESERT CONDITIONS THROUGH

DEVICE SIMULATIONS AND OUTDOOR MEASUREMENTS

Th. Katsaounis[1,3,4,*], K. Kotsovos[2], I. Gereige[2], A. Basaheeh[2], M. Abdullah[2], A. Khayat[2], E. Al Habshi[2], A. Al-Saggaf[2] and A. Tzavaras[1]

[1]Computer Electrical and Mathematical Science & Engineering (CEMSE), King Abdullah University of Science and Technology (KAUST), Thuwal, Saudi Arabia

[2]Saudi Aramco R&D Center, Carbon Management Division, Dhahran, Saudi Arabia

[3]Institute of Applied and Computational Mathematics (IACM), Foundation for Research and Technology - Hellas (FORTH), Heraklion, Greece

[4]Dept. of Math. & Applied Mathematics, Univ. of Crete, Heraklion, Greece

[*]Corresponding author: Computer Electrical and Mathematical Science & Engineering (CEMSE), KAUST, Thuwal, Saudi Arabia, email: theodoros.katsaounis@kaust.edu.sa

ABSTRACT: The Middle East region is considered as one the most promising areas for PV deployment due to its vast solar potential. Despite this fact, successful deployment of PV systems in the region is challenging due to local weather conditions. Dust storms are very frequent in these areas, which not only cause heavy soiling on PV module surface but may also significantly affect the form and intensity of the solar spectrum due to airborne dust particles which scatter sunlight. In addition, the combination of high ambient temperatures and increased irradiance levels pose additional challenges in PV module performance and reliability. Therefore, in this work a customized device simulator is proposed aiming to provide accurate calculations of PV module energy yield and performance using local climate data including solar radiation spectrum and temperature measurements. Simulation data are validated with outdoor IV measurements on various types of commercial c-Si based PV modules including polycrystalline Si and bifacial PERC, located at KAUST University at the Western Region of Saudi Arabia.Seasonal performance variations of various solar cell technologies due to local spectrum variations are also investigated.

Keywords: c-Si, Silicon Solar Cell, PERC, Bifacial, Modelling, Simulation, Performance

1 INTRODUCTION

Middle East region is considered as one the most promising regions for PV deployment due to its vast solar potential. In particular, the average annual Global Horizontal Irradiance (GHI) in Saudi Arabia is 2200 kWh/m2 [1], allowing for a very competitive energy production cost as demonstrated by the recent record-breaking bid for the Sakaka 300 MW PV project, at a tariff of 2.34 US-cents per kWh [2]. Despite this fact, successful deployment of PV systems in the region is challenging due to local weather conditions.

Dust storms are very frequent in these areas, which not only cause heavy soiling on PV module surface but may also significantly affect the form and intensity of the solar spectrum due to airborne dust particles which scatter sunlight. In addition, the combination of high ambient temperatures and increased irradiance levels pose additional challenges in PV module performance and reliability.

Therefore, in this work a customized device simulator is proposed aiming to provide accurate calculations of PV module energy yield and performance using local climate data including solar radiation spectrum and temperature measurements.

Simulation data are validated with outdoor IV measurements on various types of commercial c-Si based PV modules including polycrystalline Si and bifacial PERC, located at KAUST University at the Western Region of Saudi Arabia.

In addition, this study also focuses on the effects of spectral changes and the influence of airborne dust particles to the solar radiation incident at the PV module surface. Seasonal performance variations of various solar

cell technologies using local spectral data are also investigated.

2 DEVICE SIMULATOR MODEL

The system of carrier transport equations is solved numerically using the finite element method. An implicit-explicit variant of Newton's method is used to linearize the system and solve each equation separately thus reducing the computational cost considerably. The computational domain was covered by a triangulation, while mesh adaptivity, see Figure 1 (right), is used to resolve the Dirac-like behavior of the incident light on the cell surface as well as to capture the steep gradients of the solution around the back contact. The solver was tested and compared with various well-known open source solar cell device simulators. Further details regarding the model and its underlying mathematical formulation can be found in [3].

The solar cell device simulator also includes additional features to take into account metal grid shading, reflection and temperature effects. In particular:

• the cell surface texturing is assumed to be of pyramidal shape with 45^0 angle;

• the effect on the incident solar irradiance of the geographical location and the tilt angle of the PV module, are also considered

• the shading of metallic grid and busbar is calculated

• the reflection of the incident light from the solar cell surface and the glass of the module was taken into account

• the dependence on temperature of various device material parameters of the problem such as carrier mobility, intrinsic carrier concentration, recombination current density etc. were also considered.

Part of the code was developed using the FreeFem++ finite element computational framework [4]. The iterative scheme with mesh adaptivity converges in few iterations with a tolerance of 10^{-12} between two successive iterates. The computational time to obtain an IV-curve consisting on the average of 120 points varied from 10 − 30 min. It's remarked that the customized solver (KASCS) uses an adaptive algorithm to choose the voltage step during the calculation of an IV-curve.

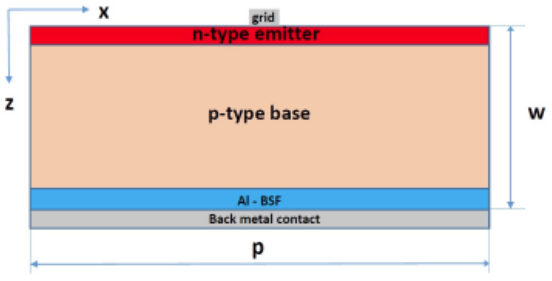

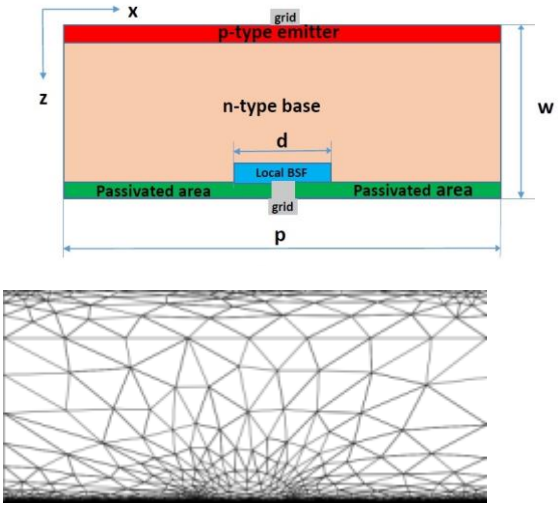

Figure 1. Geometry model of a monofacial (top), bifacial PV device (middle) and representative triangulation (bottom).

The numerous simulations were performed on the **CRAY XC40** (Shaheen) of the Supercomputing Laboratory at King Abdullah University of Science & Technology (KAUST) in Thuwal, Saudi Arabia.

3 EXPERIMENTAL SETUP

The outdoor experimental system is installed at KAUST in Thuwal, Western region of Saudi Arabia at the New Energy Oasis (NEO) test field near the Red Sea coast (22.30 N, 39.10 E). The system consists of the following components:

• A set of commercial PV modules, including polycrystalline Si and bifacial PERC, with ground mounting system

• IV measuring system with radiation sensors, industrial PC and datalogger

• Solar resource measurement station with pyranometers, spectroradiometer and sky camera

The modules selected for this study consist of a monofacial polycrystalline Si PV module and a bifacial monocrystalline Si, which are chosen to have similar electrical characteristics based on their manufacturer datasheet as shown on Table 1. The modules were installed in a standard Al profile mounting system with South facing orientation, where the system was designed to support various tilt angles. Testing was performed at 25 & 45 degrees tilt angles, with 20 cm module elevation, where the ground is paved with gray coloured gravel. Each of them was connected to an IV tracer measuring system with multiple inputs [5] in order to monitor the electrical characteristics of each one separately.

The solar resource measurement station is installed in the same outdoor field, near the site where the PV module measurement setup is located. The setup as includes four sensors to perform precise measurements of the three solar radiation components: Global Horizontal Irradiance (GHI), Direct Normal Irradiance (DNI), Diffuse Horizontal Irradiance (DHI) and the global spectral distribution (s-GHI). It also includes a sky camera to take hemispheric pictures of the sky. The system was designed and installed by TUV Rheinland [5].

PV structure	Monofacial	Bifacial
Technology	Poly -Si	Mono -Si
Cell number	60	60
P_{max} (W)	240	245
I_{sc} (A)	8.75	8.76
V_{oc} (V)	36.8	38.5
FF (%)	75.36	72.65
Efficiency (%)	14.5	15.1

Table 1. PV module specifications based on manufacturer's datasheets.

4 RESULTS

4.1 PV module temperature calculations

One of the most important factors affecting solar cell operation is temperature. In many areas of the Middle East the ambient temperature can rise several degrees above nominal conditions (25^0C) and module temperature can reach 60^0C or higher. Temperature affects several material parameters, which can considerably reduce PV module efficiency. These temperature effects are incorporated in our solar cell simulator. To evaluate module temperature, we use a group of models [6-10] with parameters which, are readily available such as air temperature, solar irradiance, wind velocity and PV module efficiency. To improve accuracy, we proceed by taking a linear combination of all aforementioned models, where the coefficients are determined by linear least square fitting to actual PV module temperature measurements. An example of fitting results is illustrated in Figure 2.

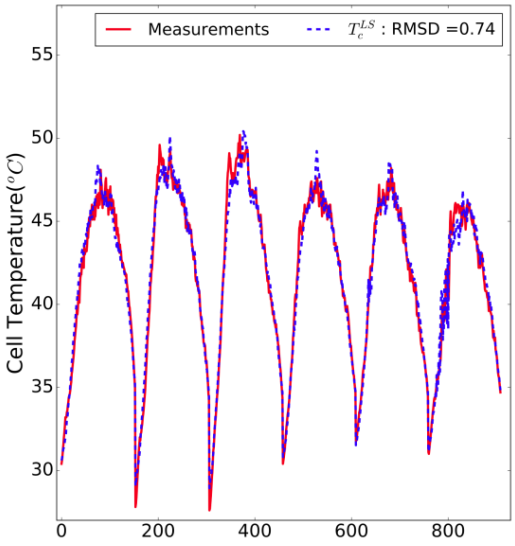

Figure 2. Least square fitting of PV module temperature models (blue curve) and actual measurements (red).

According to the estimation of PV module operating temperature described above, several material parameters affected by the temperature are modified in the model. The main focus was on parameters with significant contribution to PV module operation: Silicon light absorption coefficient ($\alpha(\lambda)$), intrinsic carrier concentration (n_i), carrier mobilities (μ_n, μ_p), recombination current density (J_0), and electron lifetime τ_n.

4.2 Local climate spectral effects

As already mentioned, dust storms are very frequent in the Middle East region, which may also significantly affect the shape and intensity of the solar spectrum due to airborne dust particles which scatter sunlight. An example is shown on Figure 3, where a comparative plot of the global sunlight spectra at noon (12: 30 pm) for three different dates is illustrated. The AM1.5 Global is also added as a reference. The spectrum on March 28th (blue curve) is received on a clear day before the sandstorm, the one on April 4th (purple curve) is after the event, while that on March 30th occurred at the peak of the event. The event induced high concentration of airborne dust particles which significantly reduced solar radiation intensity and changed spectrum shape as well as increasing dramatically the portion of the diffuse irradiance while diminishing the direct part as shown on table 2.

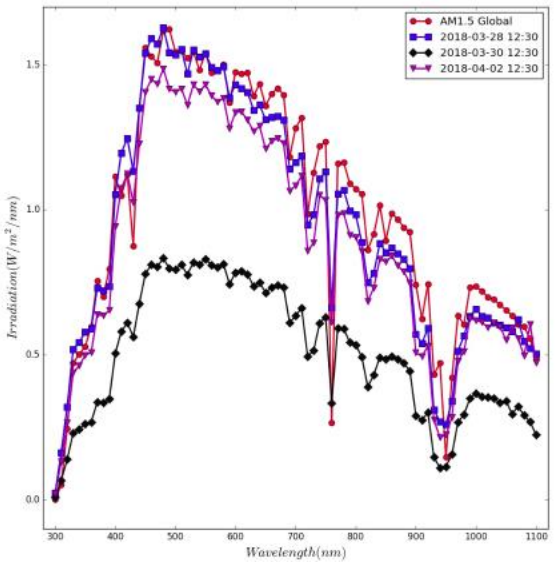

Figure 3. Local spectra measured for 3 different dates at noon (12:30 pm) with the Global AM15 added as reference (red curve)

This is evident also from the color of the sky change from blue to a yellowish tint as also shown on the sky camera snapshots of Figure 4. The spectrum comparison shows that after the sandstorm event, the intensity of the solar spectrum has been significantly reduced, especially at UV and visible wavelengths, while at near IR region (beyond 800nm) it remains almost unchanged.

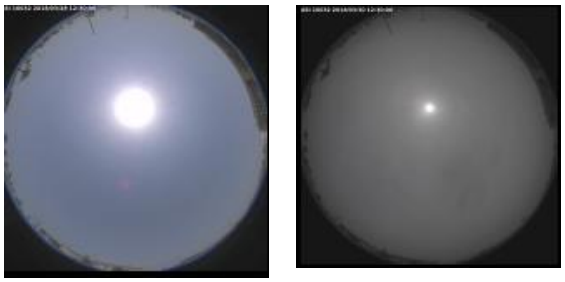

Figure 4. Sky camera snapshots at 28/03/2018 (left - before sandstorm) and at 30/04/2018 (right - shortly after the event).

The event induced high concentration of airborne dust particles which significantly reduced solar radiation intensity and changed spectrum shape as well as increasing dramatically the portion of the diffuse irradiance while diminishing the direct part as clearly shown on table 2.

Date	GHI (W/m ^{2})	DHI (W/m ^{2})	DNI (W/m ^{2})
28/03/18	941	310	669
29/03/18	785	564	233
30/03/18	479	450	31
31/03/18	520	487	35
01/04/18	874	534	357
02/04/18	872	502	387

Table 2. Solar irradiance values (global - GHI, diffuse - DHI, & direct - DNI) for the period 28/03-02/04/18 during a sandstorm event at KAUST.

Spectrum changes such as those described above also affect PV module performance as will be demonstrated in the next section.

4.3 Energy Yield comparison results

In this section we compare the electrical performance characteristics of the PV modules obtained from the simulations with the corresponding ones from measurements. Figure 5 illustrates the daily yield output (kWh/kWp) for both 25^0 & 45^0 tilt angles, where the left graphs corresponds to the monofacial module while the right ones refer to the bifacial device. Measurement period displayed for each angle respectively was 28/03/2018 - 02/04/2018 (25^0) and 23/04/2018 - 28/04/2018 (45^0). Both graphs show very good agreement between the experimental curves (red lines) and the simulated curves(black color) with the latter following exactly the measured daily energy yield changes, thus validating our model. The simulated curves are corrected by taking into account external series & shunt resistances extracted from the experimental IV curves through nonlinear least square fitting [5]. The agreement of corrected daily yield output with the experimental data is remarkable, especially for the 45^0 tilt angle thus validating the aforementioned correcting process.

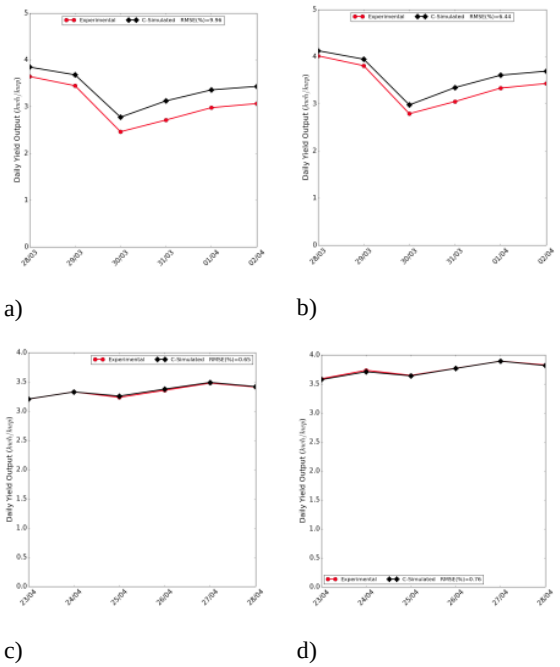

Figure 5. Daily yield output (kWh/kwp) for 25^0 (top curves) & 45^0 (bottom curves) tilt angle: Monofacial (a, c), Bifacial (b, d). Measurement period displayed for each angle respectively was 28/03/2018 - 02/04/2018 (25^0) and 23/04/2018 - 28/04/2018 (45^0).

As a final step, we compare the performance of the bifacial device with the monofacial one. Figure 6 shows the simulated and experimental relative energy gain of the bifacial module compared to the monofacial one for the 25 and 45 degree angles respectively. Measurement period displayed for the (25^0) angle was 28/03/2018 - 06/04/2018 and 23/04/2018 - 05/05/2018 for the 45^0 respectively. Both graphs show that the experimental and simulated curves are very close with each other, thus verifying the accuracy of the bifacial model simulation. The bifacial module installed at 45 degrees show slightly higher energy gain compared to the 25 degrees installation as expected due to increased irradiance on the back surface as a result of the higher tilt angle. There is a slightly above 10% energy gain of the bifacial module over the monofacial one for the 25^0 angle while the corresponding gain for the 45^0 tilt angle is about 15%.

Another aspect worth mentioning is the impact of the sandstorm event which occured during the period 29 March till April 2nd, 2018. As mentioned on the previous section, at the peak of the event on March 30th, the intensity of the solar radiation was significantly reduced as indicated on figure 3 and table 1. This resulted to a large drop in energy yield for both PV modules as expected and is clearly evident on the graphs a & b of figure 5.

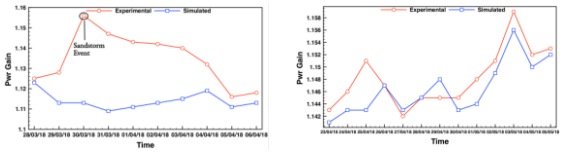

Figure 6. Bifacial daily energy yield gain for 25^0 (left) and 45^0 tilt angle (right).

On the contrary, it's observed that the energy yield gain of the bifacial module reached its maximum value during the peak of the event as shown on the left diagram of figure 6. This can be attributed to the high levels of diffused solar irradiance occurred during that period as demonstrated on table 2, which is the result of solar radiation scattering due to increased concentration of airborne dust particles. The simulated energy gain underestimated the actual measurements for this case, most probably because the radiation sensor could not measure accurately the amount of the diffused irradiance on the back of the module.

Such event did not occur during the measurement interval for the 45^0 tilt angle, where weather conditions were stable and energy yield for each module remained relatively unchanged. In this case, simulated energy yield gain was almost identical to the measured one.

In summary, the above analysis demonstrates that for the Middle East region, where dust storms are frequent, PV module performance can be significantly affected during such events.

5 CONCLUSIONS

In this study an extended analysis was presented through a series of comparisons between experimental data obtained from a set of one monofacial and a bifacial PV module installed nearby the western coast of Saudi Arabia and the results of a customized solar cell device simulator developed to take into account spectral and temperature effects. The simulated results predict very well the daily yield output for both devices. The bifacial device shows a gain of 10% and 15% for 25^0 and 45^0 tilt angle, respectively, when compared to the monofacial one.

Our results further suggest that PV installations in the Middle East region where sandstorms are frequent and their effects may last for several days, device performance can be significantly affected due to scattering of solar radiation by the airborne dust particles. It was demonstrated that during such events, the intensity of the solar spectrum was significantly reduced, while diffused radiation was dominant. This fact indicates that it would be beneficial using bifacial devices over monofacial ones since they can absorb more of the diffused sunlight which is in abundance when such phenomena occur.

ACKNOWLEDGEMENTS

The authors acknowledge the support of the Supercomputing Laboratory at King Abdullah University of Science & Technology (KAUST) in Thuwal, Saudi Arabia; the KAUST Economic development for their technical support and Saudi Aramco R&D Center - Carbon Management Division for their financial support through grant RGC#3893.

REFERENCES

[1] S. Alawaji, Renewable & Sustainable Energy Reviews 5 (2001) 59.

[2] ACWA Power wins 300MW Saudi solar project, https://www.pv-tech.org/news/acwa-power-wins-saudi-300mw-solar-project

[3] Th. Katsaounis, K. Kotsovos, I. Gereige, A. Al-Saggaf, and A. Tzavaras, Solar Energy, 158 (2017) 34.

[4] F. Hecht, J. Numer. Math, 20 (2012) 251.

[5] Th.Katsaounis, K.Kotsovos, I. Gereige, A.Basaheeh, M.Abdullah, A.Khayat, E. Al-Habshi, A.Al-Saggaf, and A.E.Tzavaras, Renewable Energy, 143 (2019) 1285.

[6] J. A. Duffie and W. A. Beckman, Solar Engineering of Thermal Processes, (2006) Wiley.

[7] J. M. Servant, Calculation of the cell temperature for photovoltaic modules from climatic data, Proceedings of the 9th biennial congress of ISES- Intersol 85, (1985).

[8] R. Chenni, M. Makhlouf, T. Kerbache, and A. Bouzid, Energy, 32 (2007) 1724.

[9] F. Lasnier and T. G. Ang, Photovoltaic engineering handbook, Adam Hilger (1990).

[10] D. L. King, W. E. Boyson, and J. A. Kratochvill, Photovoltaic array performance model (2004).